Materials Science-Poland, Vol. 25, No. 3, 2007

Computational study of the C–C interaction in the *bcc* Fe(001) inner plane containing a vacancy

S. SIMONETTI[1, 2*], A. JUAN[2], G. BRIZUELA[2]

[1]Departamento de Ingeniería Mecánica, Universidad Tecnológica Nacional, 11 de Abril 461, 8000 Bahía Blanca, Argentina

[2]Departamento de Física, Universidad Nacional del Sur, av. Alem 1253, 8000 Bahía Blanca, Argentina

The C–Fe interaction in the (001) *bcc* Fe that contaning a vacancy was analyzed using a semi-empirical theoretical method. A cluster model containing 125 atoms was used to simulate the local environment of the Fe vacancy. Carbon atoms were positioned in their local energy minima configurations. The most stable positions for the C atoms in the (001) *bcc* Fe were found at about 1.2 Å from the vacancy centre and close to the first nearest-neighbour octahedral sites. Fe atoms surrounding the vacancy weaken their bond when C is present. This bond weakening is a consequence of the C–Fe bond formation. The Fe–C interactions occur mainly via Fe 4s orbitals with a lesser participation of Fe 4p and Fe 3d orbitals. The C–C interaction was also analyzed. For the C–C distance of 1.4 Å, there is a possible bonding between the C atoms in the (001) *bcc* iron. The Fe–C interactions are stronger than the C–C interaction.

Key words: *computer simulation; vacancy; iron; carbon*

1. Introduction

Desirable reactions include the formation of carbon nanotubes from gaseous hydrocarbons, making gasoline from synthesis gas, etc. [1–3]. On the other hand, coke formation on the catalyst surface is undesirable, as it poisons the catalyst [4]. It is therefore of interest to study how isolated carbon atoms bind with Fe surfaces, as the first step towards understanding further reactions involving carbon interaction with other carbon atoms on the surface or with substrate Fe atoms to form carbide. Carbon atoms occupy octahedral positions of the *bcc* Fe lattice causing distortion due to the size of its atomic radii [5]. Mc. Lellan et al. propose that diffusing C atoms occupy tetrahedral and octahedral sites successively [6]. Grabke investigates the C adsorption and reports that most probably it occurs in the interstitial sites on the surface, each embedded between four iron atoms [7]. Jiang and Carter find that carbon atoms bind strongly with Fe surfaces and prefer high coordination sites [8].

*Corresponding author, email: ssimonet@uns.edu.ar

The presence of carbon affects electronic structure of the bulk iron ions. Anderson studied the interaction of carbon with iron surfaces and found bond weakening and rehybridization of iron orbitals [9]. Gavriljuk et al. observed that the metal-impurity interaction was limited by the local environment. The electron states localized on the second Fe neighbour were weakly influenced by the impurity [10]. Carbon impurities have been observed to interact strongly with lattice defects. The study of foreign interstitial C atoms interacting with point defects in *bcc* Fe has been reported by Domain et al. The authors reported a strong binding energy of C with the vacancy [11].

The energy of a carbon and hydrogen atoms interacting with other iron crystalline defects was investigated by our group in previous works and reported in [12–14]. We have studied the electronic structure of C and H atoms simultaneously absorbed in an (111) edge dislocation core system in *bcc* iron [12], near a stacking fault zone in *fcc* iron [13] and in the region of a bivacancy [14]. The defect zone is the preferential region for the C localization. The C acts as an expeller of H and could reduce the detrimental effect of H on the Fe–Fe bonds. The C atom has also the possibility of making a bridge between Fe atoms of different layers that could provide an additional compensation effect to the Fe matrix.

The objective of the present work is to study the interaction between one and two C atoms with a monovacancy in the (001) *bcc* Fe, including the electronic structure and bonding considerations. The (001) *bcc* Fe plane was selected for the present study because it contains the metal vacancy and the nearest interstitial sites. The theory and model considered are described in the following sections.

2. Computational method

Our calculations were performed using the ASED-MO (atom superposition and electron delocalization molecular orbital) method which predicts molecular structures from atomic data (atomic wave functions and ionisation potentials) [15–18]. The modification of the extended Hückel molecular orbital method (EHMO) was implemented with the YAeHMOP program [19]. Double zeta expansions of metal d orbitals were employed. The parameters are listed in Table 1.

Table 1. Parameters for ASED-MO calculations

Atom	Orbital	Ionization potential [eV]	Slater exponent (au-1)	Linear coefficient	Electronegativity (Pauling)
Fe	3d	9.00	5.35	0.5366	1.8
			1.80	0.6678	
	4s	7.87	1.70		
	4p	4.10	1.40		
C	2s	16.59	1.55		
	2p	11.26	1.45		

The ASED-MO is a semi-empirical method which makes a reasonable prediction of the molecular and electronic structure [20]. The ASED theory is based on a physical model of molecular and solid electronic charge density distribution functions [18–21]. The adiabatic total energy values were computed as the difference between the electronic energy (E) of the system when the impurity atom/fragment was at a finite distance within the bulk and the same energy when that atom/fragment was far away from the solid surface. There are many types of energies concerning electronic structure calculations.

The sequential carbon absorption energy can be expressed as:

$$\Delta E_{\text{total}} = E\left(Fe_m - C_n\right) - E\left(Fe_m - C_{n-1}\right) - E\left(C\right) + E_{\text{repulsion}} \tag{1}$$

where m is the size of the cluster and n is the number of carbon atoms.

The stability of the agglomeration of carbon in Fe, that is the energy difference between the agglomeration of n carbon and n single carbon atoms in Fe vacancy, was also computed as:

$$\Delta E_{\text{aggl,total}} = E\left(Fe_m C_n\right) - E\left(Fe_m\right) - n\left[E\left(Fe_m C_1\right) - E\left(Fe_m\right)\right] + E_{\text{repulsion}} \tag{2}$$

where again m is the size of the cluster and n is the number of carbon atoms.

The binding energy is the difference between the minimum adsorption energy of C impurity in the vacancy, $\Delta E(\text{C}_{\text{def}})$, and the adsorption energy of C impurity on a tetrahedral or octahedral interstitial site of the perfect Fe matrix, $\Delta E(\text{C}_{\text{int}})$. Then, it was calculated as:

$$\Delta E_{\text{binding}} = \Delta E(C_{\text{def}}) - \Delta E(C_{\text{int}}) \tag{3}$$

The repulsive energy was computed taking into account all atom–atom interactions.

To understand the interactions between the atoms, we used the concept of DOS (density of states) and COOP (crystal orbital overlap population) curves. The DOS curve is a plot of the number of orbitals per unit volume per unit energy. The COOP curve is a plot of the overlap population weighted DOS vs. energy. The integration of the COOP curve up to the Fermi level (E_f) gives the total overlap population of the bond specified and it is a measure of the bond strength.

A comment follows about the methods used in this paper. The (EH) based methods supply useful information about different aspects of the electronic structure and the chemical reactivity. The method has been successfully employed for the analysis of experimental information and their correlation with atomic data. It is a methodology that reveals the basic interactions that are responsible for chemical bonding and allows one to examine the relationship between systems with similar geometrical and compositional distributions. Another advantage of the method (and its modification) is that it allows working with systems that include hundred atoms of transition metals per unit cell. Our group has recently used this method in similar systems, computing under the ASED approximation the C and H trajectories in defects of α-Fe and γ-Fe matrices

[12–14]. Our results match qualitatively those of ab-initio calculations. The structure and properties of iron bulk and Fe alloys were calculated in order to establish the reliability of the method employed, as well as to determine suitable converged values of computational parameters to be used in the subsequent determination of the impurity position. When we compare our results obtained from the ASED method with those obtained from other theoretical methods, we can see that the results are in a good agreement. The method allows us to determine the contribution of each orbital of Fe and C atoms to the bonding. Using extended Hückel calculations we have tried to build a bridge between chemical intuition and computational theory. We are interested in understanding, trends, and occasionally predictions. The key strength of the ASED (or EH) method consists in its transparency and the main objective of the present work is to provide a qualitative picture of C atoms binding within the Fe matrix.

3. The Fe-vacancy cluster model

BCC iron has a *bcc* structure with a lattice parameter *a* of 2.861 Å and the nearest neighbour distance of 2.47 Å [22]. The cluster used to simulated solid *bcc* Fe has 125

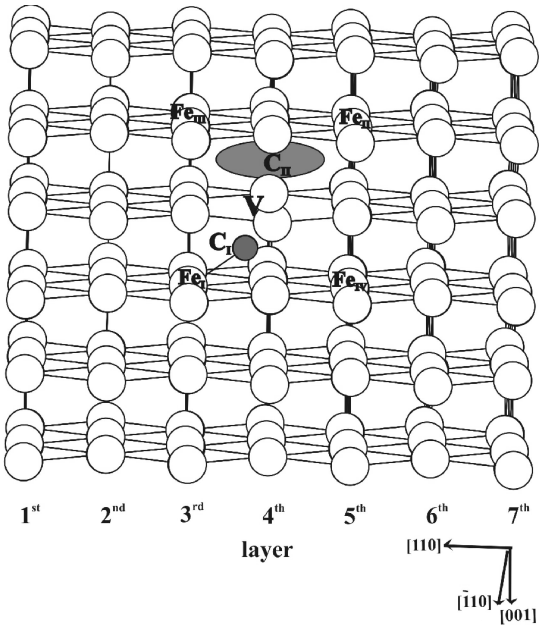

Fig. 1. Schematic view of the impurity adsorption in the (001) *bcc* Fe containing the vacancy (V). The C_I location and the favourable zone for C_{II} adsorption are indicated

atoms of Fe distributed in seven layers stacking (110) planes. The vacancy is set in the fourth layer (Fig. 1). The thickness of this slab is sufficient to approximate the electronic structure of 3D bulk Fe in the innermost layer.

We have computed the adiabatic total energy of the system absorbing up to one and two carbon atoms in the vacancy region. The impurities were located, one by one, in their positions of minimum energy. We have computed the minimum energy position for the impurities covering the entire (001) plane which contains the metal vacancy, and the nearest octahedral and tetrahedral sites. Having determined the most stable position for the impurities in the zone near the vacancy, we studied the Fe_{matrix}–C and the impurity–impurity interactions.

4. Results and discussion

4.1 The Fe_{125}–C_I system

4.1.1. Location of a carbon atom near the vacancy zone

First of all, we performed calculations for a single carbon atom (C_I) inside the cluster, finding a minimum of –13.55 eV, indicating its most stable localization in the (001) *bcc* Fe. The minimum was found at 1.72 Å of its first Fe neighbour (Fe_I). The contour lines corresponding to the energy surface for C absorbed on the region mentioned in the previous paragraph are shown in Fig. 2.

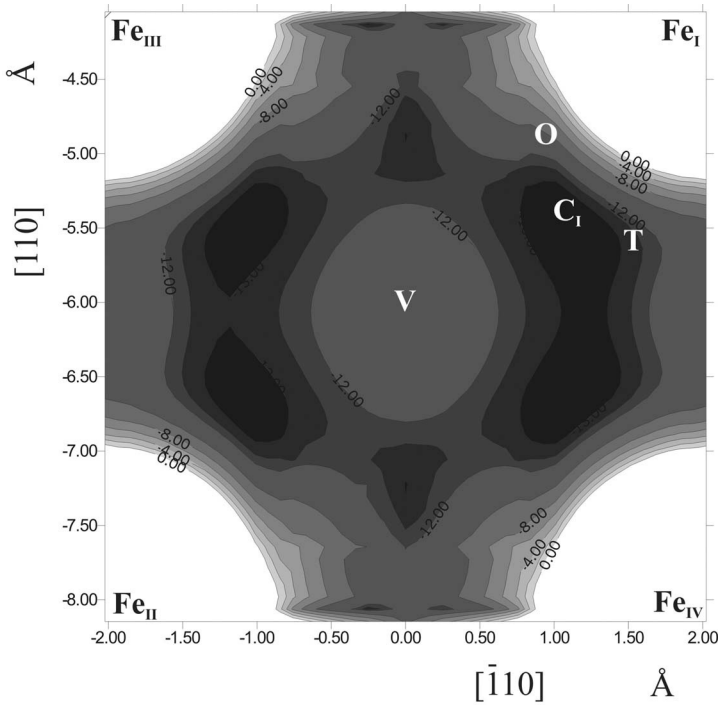

Fig. 2. Contour lines corresponding to the energy (eV) for the Fe_{125}–C_I system in the (001) plane containing the vacancy (V). The tetrahedral (T) and octahedral (O) interstitial sites are indicated

In an ab initio high level investigation of the diatomic iron carbide molecule, FeC, Tzeli and Mauridis report the C–Fe distance of 1.581 Å which agrees with the corresponding experimental one [23]. Niu et al. report the Fe–C distance near the dislocation core of 1.84 Å, using first principles methods including atomic relaxation [24]. Wu et al., while investigating the effect of C on Fe-grain boundary cohesion by first principles, found the C–Fe distance on (111) surface of 1.80 Å and 4% shorter than this value in the grain boundary environment [25]. Anderson, studying diatomic iron carbides, reported the Fe–C bond length of 1.77 Å which compares well with the Fe–C bond length of 1.82 Å in $[Fe_6C(CO)_{16}]^{2-}$ [21]. Jiang and Carter reported Fe–C distances of 1.98 Å on Fe (100) and 2.37 Å on Fe(110) [8]. On the other hand, the C minimum energy position in the vacancy region was found at 1.19 Å from the vacancy centre. Hautojärvi et al. established that during vacancy migration at 220 K, an asymmetric vacancy–carbon pair was formed, where the carbon atom was located 1.042 Å off the centre of the vacancy [26]. Domain et al. reported the vacancy–C distance of 1.142 Å from the vacancy centre [11]. Johnson and Damask reported that the carbon atom was positioned at 0.73 half-lattice constants from the vacancy centre along the <100> line, not far from the neighbouring octahedral position at the distance of one half-lattice constant [27]. In our case, the C atom was positioned at 0.389 Å and 0.508 Å from the nearest octahedral and tetrahedral sites, respectively. We also computed the binding energy (section 2) and discovered that the C minimum energy position in the zone of the monovacancy was 1.577 eV and 3.017 eV more stable than the C location on the tetrahedral and octahedral site of the perfect Fe matrix, respectively. These results showed an additional effect of trapping of the vacancy zone on the C atom.

4.1.2 Electronic structure

In Figure 3, an interaction diagram is shown. The metal d states form a band starting at –12 eV and with a bandwidth of 5 eV. A substantial number of s and p states penetrate the d band. The dispersion of s and p bands is much larger than the d band, reflecting the higher overlap between s and p orbitals and the more contracted nature of d orbitals. If we compare both the total DOS shown in Figs. 3a, b we can see that they are similar. The DOS of the Fe_{125}–C_I system is dominated by many bulk and surface Fe atoms. However, some changes could be observed in the region below the d metal band and it consists of peaks corresponding to C_I-based states. The impurity -based peaks are centred at lower energies, which represent an additional energetic stabilization in the vicinity of the vacancy. The small contribution of the impurity to DOS is due to its low concentration. Figure 3c shows the projected DOS for the C_I impurity. The value of the Fermi energy (E_f) is –8.138 eV. As expected, we found no significant change in the E_f. The total DOS is dominated by the Fe matrix, so that the changes are small.

Carbon affects the states of its nearest neighbour metallic bonds. The number of Fe atoms involved in the Fe–Fe bond closer to C_I. Fe_I–Fe_{nn} OP decreases to about 62%

when the C_I atom is present (Table 2). This bond weakening is a consequence of a strong C_I–Fe_I interaction. The COOP curves in Fig. 4, corresponding to the C_I–Fe_I interaction, represent bonding and antibonding peaks and the integration up to the E_f gives the total OP for the C–Fe bonding. Then, the C_I–Fe_I bonding is formed with an OP of 0.633.

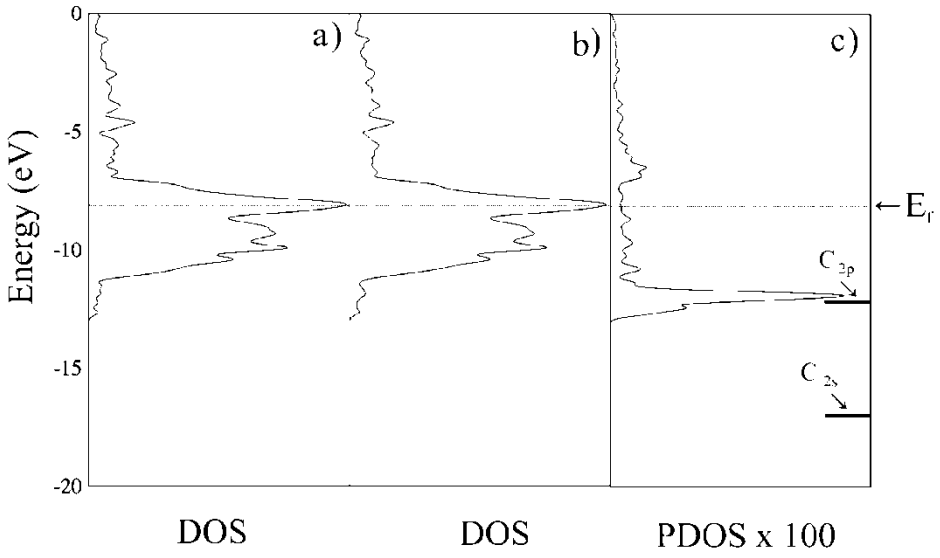

Fig. 3. Total DOS for the isolated Fe cluster (a), total DOS for the Fe_{125}–C_I cluster (b) and projected DOS for the C_I atom in the Fe_{125}–C_I cluster (c)

Table 2. Atomic orbital occupations and net charges for the C atoms and their neighbouring Fe atoms as well as the corresponding OP values for these atoms

Atom	s	p	d	Charge	Bond	OP
C_I	1.550	3.779[a]		–1.329[a]	C_I–Fe_I	0.633[a]
	1.546	3.702[b]		–1.248[b]		0.636[b]
C_{II}	1.543	3.704[b]		–1.247[b]	C_{II}–Fe_{II}	0.683[b]
Fe_I	0.606	0.272	5.616[a]	1.507[a]	C_I–C_{II}	0.050[b, c]
	0.605	0.273	5.641[b]	1.480[b]		0.021[b, d]
	0.709	0.280	5.854[e]	1.157[e]	Fe_I–Fe_{Inn}	0.116[a]
						0.115[b]
Fe_{II}	0.694	0.293	5.730[a]	1.283[a]		0.302[e]
	0.587	0.281	5.420[b]	1.711[b]		
	0.694	0.292	5.718[e]	1.297[e]	Fe_{II}–Fe_{IInn}	0.102[b]
						0.298[e]

[a]In the Fe_{125}–C_I system.
[b]In the Fe_{125}–C_I–C_{II} system.
[c]Corresponding to the C–C distance of 1.40 Å.
[d]Corresponding to the C–C distance of 2.40 Å.
[e]In the isolated Fe_{125} system.

The Fe_I 4s population decreases to about 14% when the C_I impurity is present. This indicates a participation of Fe_I 4s orbitals in the C_I–Fe_I bondings. The contribution of Fe_I 4p and Fe_I 3d populations decrease to about 3% and 4%, respectively. Some Fe–Fe bonding states are pushed up to just below the E_f. There is an electron transfer of $0.35e^-$ to the impurity from its nearest Fe neighbours. Domain et al. report that the only charge transfer clearly visible is between the C atom and its first neighbours [11].

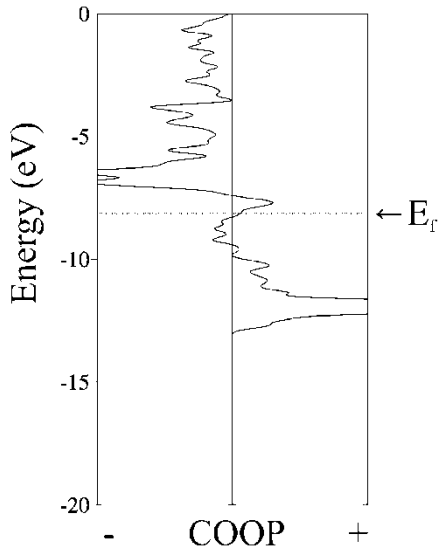

Fig. 4. COOP curves for C_I–Fe_I in the Fe_{125}–C_I system

A charge of about $0.53e^-$ was reported for interstitial C in Fe clusters located at octahedral sites of the lattice [33]. Ellis et al., studying the diffusion properties in the interstitial Cu–C solid solutions with embedded cluster density functional calculations, determined that the C acts as an acceptor of electrons in Cu, when an isolated interstitial C is placed at different sites in the lattice. The charge transfer comes from its nearest neighbours [34]. Niu et al. studying the electronic effect in dislocation core system with the presence of a C atom in the *bcc* Fe found that there were charge transfers of 0.68 e^- from the adjacent Fe atoms to the C atom and strong hybridizations occured between the C 2s, 2p orbitals and the Fe 4s, 4p orbitals [24]. In the present study, the impurity develops a negative charge while the closest Fe atoms obtain more positive charge. The additional electron from the carbon atom occupies an Fe–Fe antibonding level near E_f. So, the Fe–Fe antibonding states are now populated and it is due to the increase in E_f with respect to the clean cluster. There is less bonding due to greater participation of the Fe 4s orbital in the Fe-impurity bondings. The charge and the electron densities of the atoms involved in the interactions are summarized in Table 2.

4.2. The Fe_{125}–C_I–C_{II} system

4.2.1. Location of the second carbon atom near the vacancy zone

In the second stage, we performed calculations for an additional C atom (C_{II}) in the (001) *bcc* Fe that contains a vacancy. The fixed first C atom (C_I) resides in its minimum position (as described above), while C_{II} is moved along the vacancy region. Figure 5 shows the energy contour plot for the Fe_{125}–C_I–C_{II} system. We can see that there is a region of minimum energy for C_{II} adsorption. The vacancy offers much more room to accommodate the interstitial C atoms. Considering this zone, the shorter distances of the equilibrium C_I–C_{II} interactions are within the typical covalent bond length for C (1.38–1.48 Å for sp^2 bonds [30]). On the other hand, the minimum energy for C_{II} location corresponds to –13.17 eV at a longer C_I–C_{II} distance of 2.42 Å.

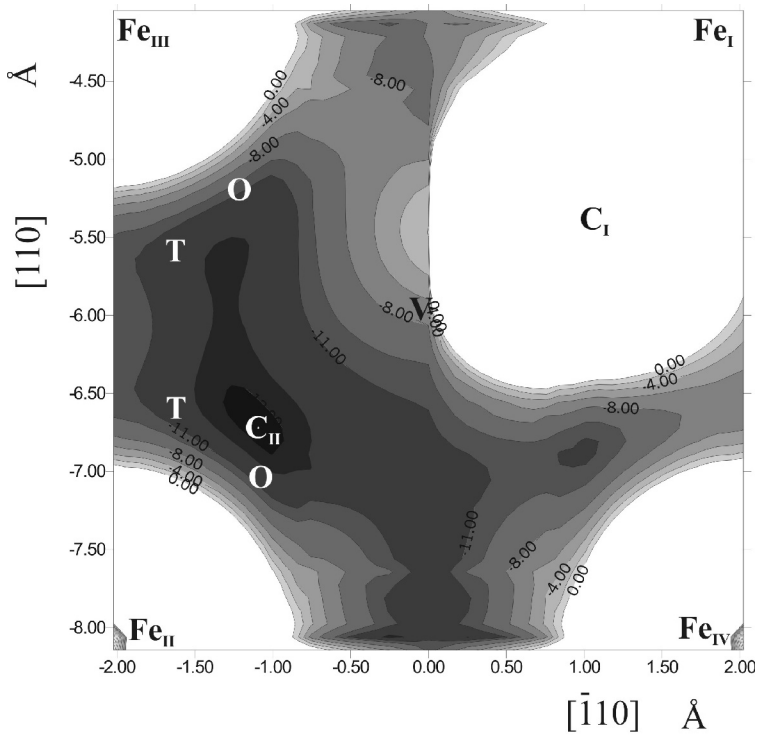

Fig. 5. Contour lines corresponding to the energy (eV) for the Fe_{125}–C_I–C_{II} system in the (001) plane containing the vacancy (V). The region for C_{II} location is shown in dark. The tetrahedral (T) and octahedral (O) interstitial sites are indicated

The minimum C_{II}–Fe_{II} distance for this configuration is 1.68 Å. Similarly to C_I, the C_{II} atom was also finally located at 0.523 Å and 0.335 Å from the nearest tetrahedral and octahedral sites, respectively; and the distance of 1.23 Å from the vacancy centre. The most stable configuration in the plane (001) corresponds to both C atoms

occupying the vacancy zone near the first nearest-neighbour octahedral sites. The agglomeration energy (section 2) was also analyzed. According to our calculations, the energy of two C atoms associated with one vacancy is close to the energy of one C atom with a vacancy. This result indicates that for C there exists, with a high probability, a competition between the formation of another C–V pair and the formation of a $V–C_2$ complex. Takaki et al. found that monovacancies are nuclei for small clusters containing a limited amount of C atoms [31]. Domain et al. found that a vacancy can bind to up to two C atoms only, in a configuration where both C atoms occupy first nearest-neighbour octahedral sites whose shortest distances are perpendicular to each other [11]. Other results show that the kinetics are clearly bimolecular, indicating that only one carbon atom associates with each vacancy [32]. Under normal conditions and even under irradiation, the vacancy concentration in Fe is smaller than the C atom concentration (for pure Fe or Fe alloys), and a large proportion of the vacancies may be associated with one or two C atoms, with strong binding energies.

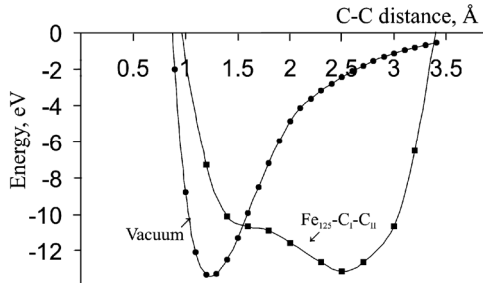

Fig. 6. Adiabatic total energy vs. C–C distance in the (001) plane containing the vacancy and under vacuum

The energy of the system was also computed as a function of the C–C distance. The C_{II} atom was moved along a line as path connecting to the C_I in order to check the stability of the system (Fig. 6). The system was more stable for C–C distances between 1.0 Å and 3.3 Å. The curve represents two relative minimums near 1.4 Å and 2.4 Å, respectively, that belong to the minimum energy region for C_{II} location previously analyzed. The region of minimum energy for C_{II} adsorption shown in Fig. 5 corresponds to C–C distances between 1.3 and 3.1 Å in Fig. 6. As a comparison, we have also obtained the adiabatic total energy curve corresponding to the C–C interaction in the vacuum (Fig. 6). The equilibrium C–C distance in the vacuum (within the ASED-MO approximation) is 1.20 Å with an energetic minimum of –13.32 eV. System stability in the Fe cluster is similar to the corresponding under vacuum.

4.2.2. Electronic structure

When two C atoms are considered, again the total DOS curves are similar to those obtained for the free cluster, as can be observed in the comparison of Fig. 7a, b. Two peaks emerge below the d metal band and this corresponds to a density of states coming from C atom states, as can be seen in Figs. 7c, d. The value of E_f is –8.134 eV.

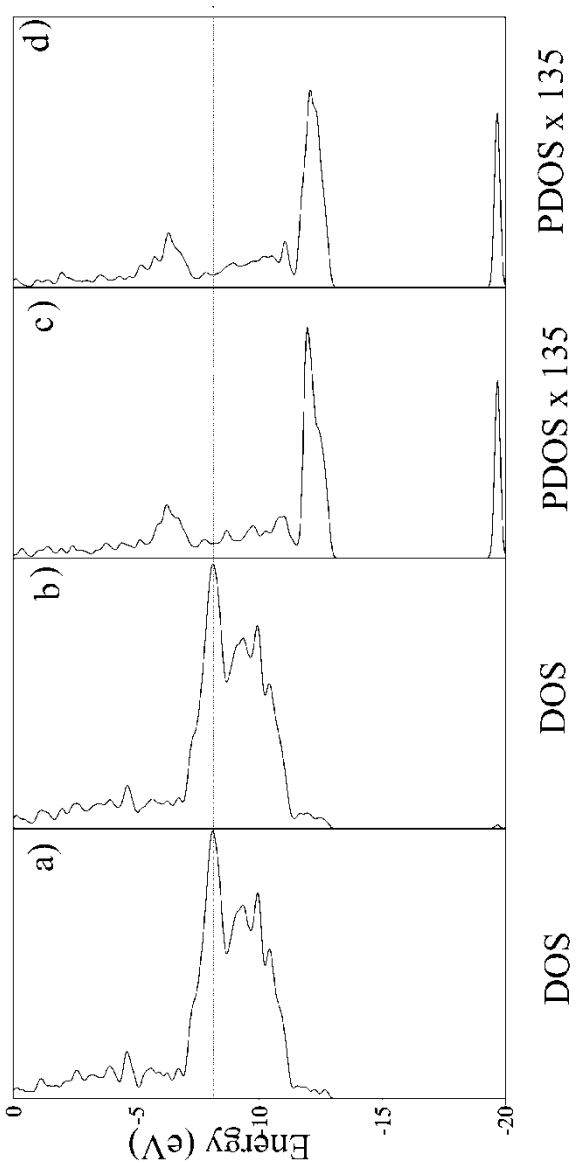

Fig. 7. Total DOS for the isolated Fe cluster (a), total DOS for the Fe_{125}–C_I–C_{II} cluster (b), projected DOS for the C_I atom in the Fe_{125}–C_I–C_{II} cluster (c) and projected DOS for the C_{II} atom in the Fe_{125}–C_I–C_{II} cluster (d)

Again, a C–Fe bonding is achieved at the expense of the Fe–Fe nearest neighbours bond. COOP curves in Figs. 8a, b show this behaviour. The interaction is almost bonding except for a region close to E_f. The OP for the C_{II}–Fe_{II} bond is 0.683 (Table 2). The interstitial C_{II} atom affects the electronic states of its surrounding Fe atoms causing a rearrangement of the electronic densities. The Fe_{II} s population decreases to about 15% while the Fe_{II} p and d populations decreases to about 4% and 5%, respectively. There is an electron transfer of about $0.43e^-$ to the C_{II} atom from the Fe_{II}. From the charge density, one can obtain a direct understanding of the interatomic bonding characteristics. The charge distribution characteristics indicate strong interactions between C and their Fe nearest neighbour atoms as well as the covalent-like bonds formed therein. As a consequence, the OP between the iron atoms near the C atom decreases. The OP for the closer Fe_{II}–Fe_{IInn} bond decreases by nearly 66%. The metal–metal bonds are then weakened.

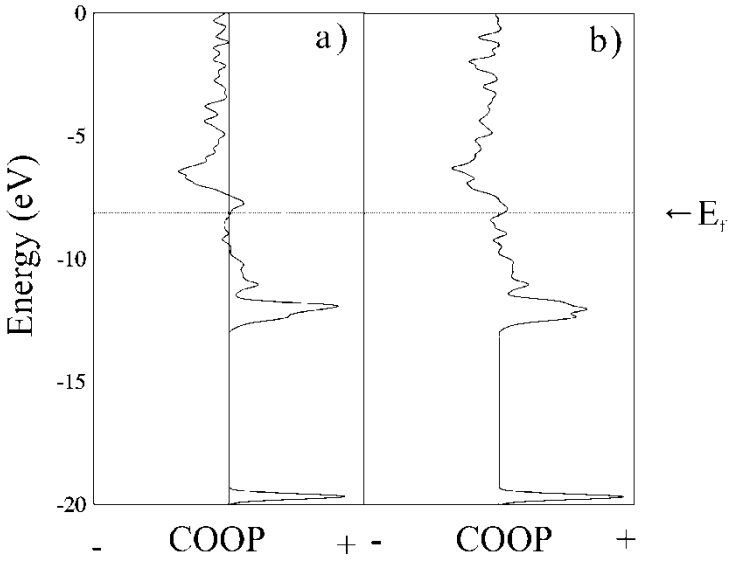

Fig. 8. COOP curve in the Fe_{125}–C_I–C_{II} system for:
a) C_I–Fe_I interaction, b) C_{II}–Fe_{II} interaction

When C_{II} is located in the Fe_{125}–C_I cluster, it practically does not affect the C_I electronic states. The addition of the C_{II} atom has a minor effect on the C_I–Fe_I bond. The C_I–Fe_I OP remains almost unchanged while the second carbon atom bonds to its closest Fe atom. The C_I becomes a bit more strongly bonded to Fe_I. The C_I–Fe_I OP increases to about 0.5% (see Table 2). In the same way, the bond strength between Fe pairs next to C_I almost does not decrease any further by the introduction of a second C. Instead, the Fe–Fe bonds close to C_{II} weaken in a similar way Fe_I–Fe_{Inn} had upon introduction of the first C atom. Then, no additional decohesion is observed in the Fe–Fe bonds when the second C atom is present but in this case more Fe–Fe bonds are af-

fected. It is observed that the charge and electronic structure of more distant iron atoms are almost unaffected by the C atoms. We thus believe their influence is limited to their first neighbours.

Considering the region of minimum energy for C_{II} location, there is a set of possible C–C associations. As we mentioned before, the minimum distances between the C atoms are around the typical covalent bond length for C and the impurity–impurity interactions are feasible. We found a small bonding between the C atoms in the (001) plane. Considering the two relative minima shown in Fig. 6, the C–C OP value is 0.050 at a C–C distance of 1.4 Å, while for a diatomic C–C in vacuum it is 0.50 and the C–C OP value is 0.021 at a C–C distance of 2.4 Å with an OP of 0.31 in the vacuum. Very low C–C OPs are a direct consequence of the metal matrix that populates antibonding C–C states at energies closer to E_f. Then, the C–C interaction on the vacancy region is small. At the same time, each C atom prefers to be bonded to the neighbouring Fe atoms. Subsequently, the Fe–C interactions are stronger than the C–C interaction.

5. Conclusions

The electronic structure of carbon in the (001) *bcc* iron with a vacancy has been studied by the ASED-MO cluster calculations. First, we included a C atom near the vacancy and then, the addition of a second C atom was analyzed.

The minimum energy positions of C atoms in the (001) *bcc* Fe were found at ca. 1.2 Å from the vacancy centre. The most stable configurations correspond to both C atoms occupying the vacancy zone near the first nearest-neighbour octahedral sites.

The addition of a C atom in the Fe matrix that contains a vacancy diminishes the strength of the local Fe–Fe bond to about 62% of its original bulk value, and by further 4% when the second C is located. This bond weakening is a consequence of a strong C–Fe interaction. The Fe–C bonds are formed at the expense of the Fe–Fe neighbour bonds. There is an electron transfer to C atoms from their Fe nearest neighbours. The Fe–C interactions occur mainly via Fe 4s orbitals with a lesser participation of Fe 4p and Fe 3d orbitals.

When two C atoms are located near the vacancy, the results are qualitatively similar to that obtained for only one C atom, that is, each C atom bonds to the surrounding Fe. No additional decohesion is observed in the Fe–Fe bonds, however in this case more Fe–Fe bonds could be affected. The C–Fe interaction is much stronger than the C–C interaction. Our results indicate that for C there exists, with a high probability, a competition between the formation of another C–V pair and the formation of a $V–C_2$ complex.

Acknowledgements

Our work was supported by the Departamento de Ingeniería Mecánica UTN-FRBB, Departamento de Física UNS, PIP–CONICET, Fullbright Commission and Guggenheim Foundation. The authors are members of CONICET.

References

[1] NISHIMURA K., OKAZAKI N., PAN L., NAKAYAMA Y., Jpn. J. Appl. Phys. Part 2, 43 (2004), L471.
[2] SCHAPER A., HOU H., GREINER A., PHILLIPP F., J. Catal., 222 (2004), 250.
[3] ANDERSON R., *The Fischer–Tropsch Synthesis*, Academic Press, Orlando FL, 1984.
[4] MEIMA G., MENON P., Appl. Catal. A, 212 (2001), 239.
[5] FROMM E., HÖRZ G., Inter. Met. Rev., 256 (1980), 5.
[6] MC LELLAN R., ISHIBACHI I., Trans. AIM., 233 (1985), 1938.
[7] GRABKE H., Mater. Sci. Eng., 42 (1980), 91.
[8] JIANG D. E., CARTER E. A., Phys. Rev. B, 71 (2005), 045402.
[9] ANDERSON A., Phys. Chem., 99 (1977), 696.
[10] GAVRILJUK V.G., KUCHERENKO YU N., MORAVETKI V.I., NADUTOV V.N., SHELUDCHENKO L.M., J. Phys. Chem. Solids, 55 (1994),1181.
[11] DOMAIN C., BECQUART C.S., FOCT J., Phys. Rev. B, 69 (2004), 144112.
[12] SIMONETTI S., PRONSATO E., BRIZUELA G., JUAN A., Appl. Surf. Sci., 217 (2003), 56.
[13] SIMONETTI S., MORO L., GONZALEZ E., BRIZUELA G., JUAN A., Int. J. Hydrogen Energy, 29 (2004), 649.
[14] SIMONETTI S., MORO L., BRIZUELA G., JUAN A., Int. J. Hydrogen Energ., 31 (2006), 1318.
[15] HOFFMANN R., LIPSCOM W., J. Chem. Phys., 36 (1962), 2179.
[16] HOFFMANN R., J. Chem. Phys., 39 (1963), 1397.
[17] WHANGBO M., J. Amer. Chem. Soc., 100 (1978), 6093.
[18] ANDERSON A., J. Chem. Phys., 62 (1975), 1187.
[19] LANDRUM G., GLASSEY W., *Yet Another extended Hückel Molecular Orbital Package (YAeHMOP)*, Cornell University, 2004.
[20] ANDERSON A., HOFFMANN R., J. Chem. Phys., 60 (1974), 4271.
[21] ANDERSON A., J. Electroanal. Chem. Interf. Electrochem, 280 (1990), 37.
[22] WYCKOFF R., *Crystal Structures*, 2nd Ed., Interscience, New York, 1963.
[23] TZELI D., MAVRIDIS A., J. Chem. Phys., 116 (2001), 4901.
[24] NIU Y., WANG S., ZHAO D., WANG C., J. Phys.: Condens. Matter, 13 (2001), 4267.
[25] WU R., FREEMAN A., OLSON G., Phys. Rev. B, 53 (1996), 7504.
[26] HAUTOJÄRVI P., JOHANSSON J., VEHANEN A., YLI-KAUPPILA J., MOSER P., Phys. Rev. Lett., 44 (1980), 1326.
[27] JOHNSON R. A., DAMASK A. C., Acta Metall., 12 (1964), 443.
[28] ROSATO V., Acta Metall., 37 (1989), 2759.
[29] RUDA M., FARKAS D., ABRIATA J., Scr. Mater., 46 (2002), 349.
[30] MARCH J., *Advanced Organic Chemistry*, Wiley, New York, 1985.
[31] TAKAKI S., FUSS J., KUGLER H., DEDEK U., SCHULTS H., Radiat. Eff., 79 (1983), 87.
[32] ARNDT R.A., DAMASK A.C., Acta Metall., 12 (1964), 341.
[33] GONG X., ZENG Z., ZHENG Q., J. Phys.: Cond. Matter. J. Phys.: Condens. Matter, 1 (1989), 7577.
[34] ELLIS D.E., MUNDIM K.C., FUKS D., DORFMAN S., BERNER A., Philos. Mag. B, 79 (1999), 1615.

Received 22 June 2006
Revised 20 March 2007